

See discussions, stats, and author profiles for this publication at: <https://www.researchgate.net/publication/263002691>

Double-Doping Approach to Enhancing the Thermoelectric Figure-of-Merit of n-Type Mg₂Si Synthesized by Use of Spark Plasma Sintering

ARTICLE *in* JOURNAL OF ELECTRONIC MATERIALS · DECEMBER 2013

Impact Factor: 1.8 · DOI: 10.1007/s11664-013-2944-x

CITATIONS

3

READS

55

8 AUTHORS, INCLUDING:



Saravanan Muthiah

National Physical Laboratory - India

14 PUBLICATIONS 98 CITATIONS

SEE PROFILE



S. Bathula

National Physical Laboratory - India

40 PUBLICATIONS 137 CITATIONS

SEE PROFILE



Kriti Tyagi

National Physical Laboratory - India

13 PUBLICATIONS 31 CITATIONS

SEE PROFILE



Ajay Dhar

National Physical Laboratory - India

65 PUBLICATIONS 598 CITATIONS

SEE PROFILE

Double-Doping Approach to Enhancing the Thermoelectric Figure-of-Merit of *n*-Type Mg₂Si Synthesized by Use of Spark Plasma Sintering

SARAVANAN MUTHIAH,^{1,2} B. SIVAIAH,¹ B. GAHTORI,¹ K. TYAGI,¹
A.K. SRIVASTAVA,¹ B.D. PATHAK,² AJAY DHAR,^{1,3} and R.C. BUDHANI¹

1.—CSIR-National Physical Laboratory, CSIR-Network of Institutes for Solar Energy, Dr K.S. Krishnan Marg, New Delhi 110012, India. 2.—Department of Mechanical Engineering, Delhi Technological University, Delhi, India. 3.—e-mail: adhar@nplindia.org

We report significant enhancement of the thermoelectric figure-of-merit of Mg₂Si by double-doping with a combination of Bi, Pb, and Sb as doping elements. Addition of any two of these three elements to Mg₂Si increases the electrical conductivity by more than three orders of magnitude at 323 K, irrespective of the doping elements used. However, a corresponding decrease in the Seebeck coefficient is observed in comparison with undoped Mg₂Si. Irrespective of the combination of the three elements used for double doping, a figure-of-merit of approximately 0.7 at 873 K is obtained for Mg₂Si; this is primarily because of enhancement of the electrical conductivity.

Key words: Mg₂Si, spark plasma sintering, double doping, thermoelectric properties, figure-of-merit

INTRODUCTION

Harnessing solar energy by use of a thermoelectric material depends both on its thermoelectric figure-of-merit and on the abundance and cost effectiveness of its constituent materials. In this regard, the specific conversion efficiency of magnesium silicide and the abundance of magnesium and silicon in the earth's crust, and hence their low cost, add to the advantages of Mg₂Si over other compounds and make it a promising thermoelectric material.^{1,2} Substitution of Mg₂Si with different dopant elements, both *p*-type and *n*-type, has been reported to lead to substantial enhancement of its figure-of-merit, primarily because the nature of the doping elements and the bonding energy involved alter the thermoelectric properties of the doped Mg₂Si.^{3–19} Recently, Liu et al.¹⁶ enhanced the thermoelectric properties of Mg₂Si_{1–x}Sn_x alloy by addition of a trace amount of Sb. Investigations have shown that the effect of doping Mg₂Si with group VA elements^{3,4} leads to better thermoelectric

properties than doping with other elements, including rare earth elements.^{7,11}

In this work, synthesis of *n*-type Mg₂Si_{0.98}Pb_{0.01}Sb_{0.01}, Mg₂Si_{0.98}Pb_{0.01}Bi_{0.01}, and Mg₂Si_{0.98}Bi_{0.01}Sb_{0.01} was achieved by mixing the constituent elements in the appropriate stoichiometric ratio then reaction by spark plasma sintering. Spark plasma sintering conditions, for example pressure, temperature, heating rate, and holding time, were optimized to furnish a single-phase material. The electrical and thermal transport properties of these double-doped Mg₂Si compounds were compared with those of their undoped counterpart. The figure-of-merit (*ZT*) was calculated by use of the formula $\alpha^2\sigma/\kappa$, where α , σ , and κ are the Seebeck coefficient (or thermopower), electrical conductivity, and thermal conductivity, respectively. It was observed that addition of any two of the doping elements Bi, Sb, and Pb to Mg₂Si increased its electrical conductivity, irrespective of the doping elements, although a decrease in the Seebeck coefficient compared with undoped Mg₂Si was also observed. The microstructure of undoped and double-doped Mg₂Si was characterized by scanning electron microscopy (SEM) with energy-dispersive spectroscopic (EDS) micro-analysis.

(Received June 28, 2013; accepted December 5, 2013)

Published online: 07 January 2014

EXPERIMENTAL

High-purity Mg (99.95%), Si (99.999%), Pb (99.95%), Sb (99.8%), and Bi (99.5%) powders were weighed in the appropriate stoichiometric proportions ($\text{Mg}_2\text{Si}_{0.98}\text{Pb}_{0.01}\text{Sb}_{0.01}$, $\text{Mg}_2\text{Si}_{0.98}\text{Pb}_{0.01}\text{Bi}_{0.01}$, and $\text{Mg}_2\text{Si}_{0.98}\text{Bi}_{0.01}\text{Sb}_{0.01}$) and milled in a high-energy ball mill (Pulverisette-4; Fritsch, Idar-Oberstein, Germany), with a 15:1 ball-to-powder ratio, in an argon atmosphere. Before sintering, the ball-milled alloy powders were handled in glove box (MB20; Mbraun, Garching, Germany) to avoid oxidation and other atmospheric contamination. The resulting mixed powders were then subjected to spark plasma sintering at 993–1053 K under vacuum (~ 4 Pa) for 10 min at a pressure of 60 MPa in a high-strength graphite die. The density of the sintered samples was found to be more than 99% of their theoretical value. X-ray diffraction (XRD) analysis was performed with a Miniflex-II x-ray diffractometer (Rigaku, Tokyo, Japan) using monochromatic Cu-K α radiation. Analysis of the microstructure of undoped and doped Mg_2Si was performed by SEM (EVO MA10; Zeiss, Jena, Germany) with an attached EDS system. For measurement of electrical conductivity and Seebeck coefficient, rectangular specimens were cut from the centre of the sintered material by use of a wire-cut saw (Model 850; South Bay Technology, San Clemente, CA, USA). Electrical conductivity and the Seebeck coefficient were measured by the four probe DC method in a helium atmosphere by use of an Ulvac-Riko (Yokohama, Japan) model ZEM-3 apparatus up to 873 K. A circular disc specimen with a diameter of 12.7 mm was used for thermal diffusivity measurement by use of a Linseis (Selb, Germany) model LFA 1000, laser flash thermal analyser under vacuum. The specific heat capacity (C_p) was measured by differential scanning calorimetry (model DSC 1; Mettler Toledo, Schwerzenbach, Switzerland). The thermal conductivity was calculated as the product of diffusivity (D), specific heat capacity (C_p), and density (ρ), i.e. $\kappa = D \times C_p \times \rho$.

RESULTS AND DISCUSSION

Figure 1 shows the XRD patterns of undoped and double-doped Mg_2Si after spark plasma sintering. XRD analysis of the samples revealed the present of trace amounts of MgO, which is formed as a by-product during the sintering process and has also been observed in previous studies of Mg_2Si .^{5,11} No other significant impurity phases were observed. Figure 2a–d shows the back-scattered SEM images of undoped and double-doped Mg_2Si . The white areas are dopant-rich regions. The microstructure of undoped Mg_2Si is characterised by random distribution of grains with no distinct grain boundaries (Fig. 2a). The doped Mg_2Si has a uniform microstructure with distinct sub-grain and grain boundaries, irrespective of the doping elements used (Fig. 2b–d). The grain size distribution of undoped and doped Mg_2Si seems to be uniform. The surface morphology of the doped Mg_2Si shows evidence of

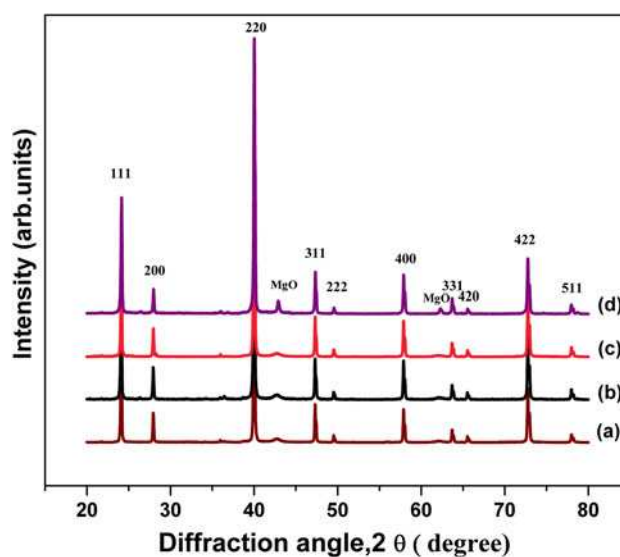


Fig. 1. XRD patterns of sintered Mg_2Si . (a) undoped, (b) Pb and Bi-doped, (c) Pb and Sb-doped, and (d) Sb and Bi-doped.

distinct grains and sub-grains with ultrathin boundaries of different constituent elements. The EDS analysis suggests that the doping elements are incorporated partly into the grains and partly into the grain boundaries. Significant enhancement of the electrical conductivity of doped Mg_2Si is probably because of addition of metallic or semi-metallic dopants which result in the distinct, uniform stable microstructure.

The temperature-dependent electrical conductivity of undoped and double-doped Mg_2Si is shown in Fig. 3. The electrical conductivity of double-doped Mg_2Si is substantially enhanced; the increase is approximately 60-fold compared with undoped Mg_2Si at the highest temperature, irrespective of dopant combination. At 873 K, the electrical conductivity increases from ≈ 1327 S/m to 60000 S/m after double doping with Pb and Sb. Moreover, the electrical conductivity of double-doped Mg_2Si is much higher than that reported for Mg_2Si single-doped with Te,⁵ Al,⁶ or Y.⁷ It can be inferred from Fig. 3 that metallic-type conductivity is observed for double-doped Mg_2Si whereas semiconducting behaviour is observed for undoped Mg_2Si . The metallic and/or semi-metallic inclusions in the Mg_2Si participate in enhancing the electrical conductivity of double-doped Mg_2Si . The temperature-dependent Seebeck coefficient of undoped and double-doped Mg_2Si is shown in Fig. 4. It is clear from Fig. 4 that, in contrast with the undoped material, all three combinations of double doping used in this study result in a similar increase in the Seebeck coefficient with increasing temperature. The repeatability of electrical conductivity and Seebeck coefficient values of Pb and Sb-doped Mg_2Si was confirmed by conducting experiments in both heating and cooling modes (Fig. 5).

The thermal conductivity of undoped and double-doped Mg_2Si as a function of temperature is shown

Double-Doping Approach to Enhancing the Thermoelectric Figure-of-Merit of *n*-Type Mg_2Si Synthesized by Use of Spark Plasma Sintering

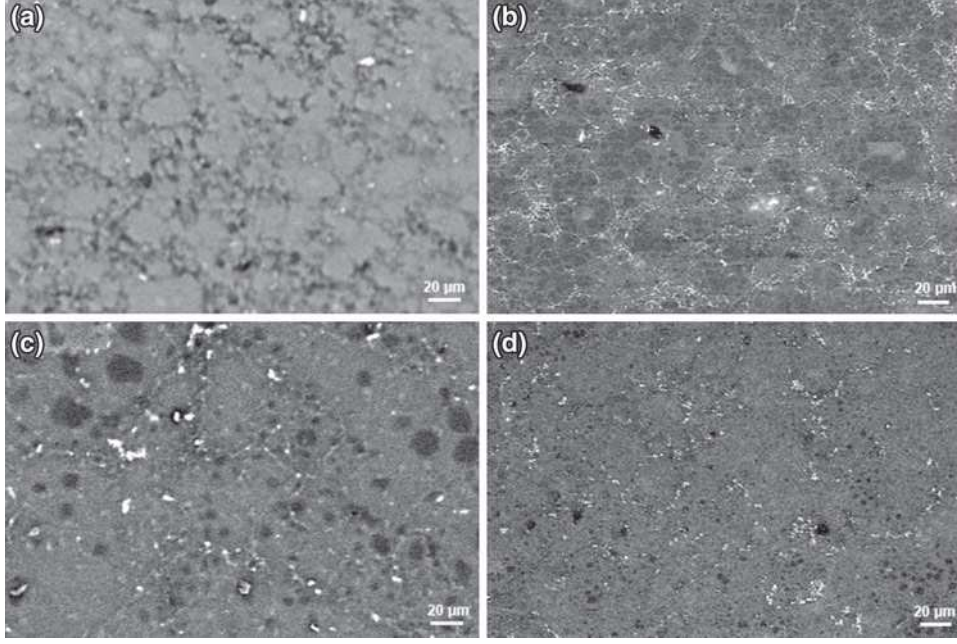


Fig. 2. SEM images of sintered Mg_2Si . (a) undoped, (b) Pb and Sb-doped, (c) Pb and Bi-doped, and (d) Sb and Bi-doped.

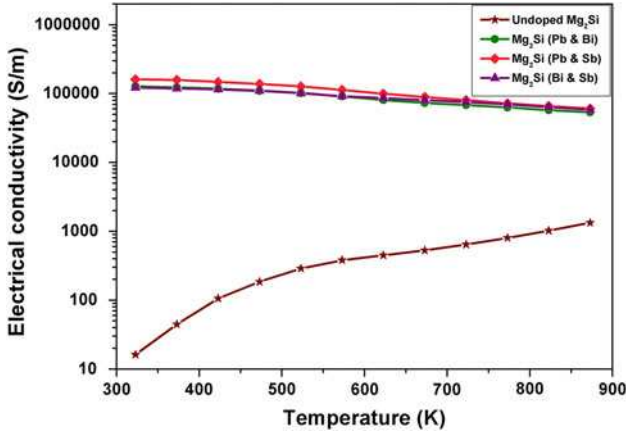


Fig. 3. Temperature dependence of the electrical conductivity of undoped and double-doped Mg_2Si .

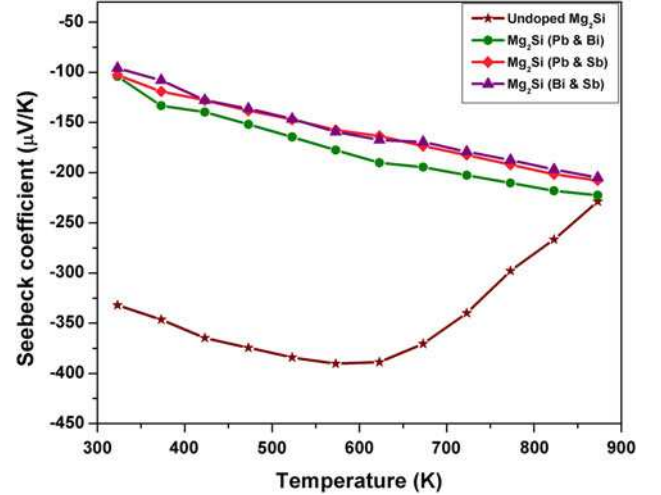


Fig. 4. Temperature dependence of the Seebeck coefficient of undoped and double-doped Mg_2Si .

in Fig. 6. At 873 K, the thermal conductivity of undoped Mg_2Si is $\sim 2.2 \text{ W/mK}$, which is lower than that of double-doped Mg_2Si ($\sim 3 \text{ W/mK}$). The lattice thermal conductivity (κ_{ph}) values were estimated by subtracting the electronic thermal conductivity (κ_{el}) from κ_{total} , obtained by use of the Wiedemann–Franz law with Lorenz number $L = 2.45 \times 10^{-8} \text{ V}^2/\text{K}^2$. The inset in Fig. 6 shows that the temperature dependence of lattice thermal conductivity is quite similar for all the double-doped and undoped Mg_2Si samples, with the major contribution to the total thermal conductivity arising from the lattice thermal conduction, for all the samples.

The temperature-dependent power factor for undoped and double-doped Mg_2Si is shown in Fig. 7. The power factor of undoped Mg_2Si has a maximum

value of $6.9 \times 10^{-5} \text{ W/mK}^2$ which increases on double doping to $262 \times 10^{-5} \text{ W/mK}^2$ at 873 K. Although there is a substantial reduction in the Seebeck coefficient (α), the significant increase in electrical conductivity (σ) is vital in enhancing the power factor ($\alpha^2\sigma$). Our findings confirm that almost similar power factor values are obtained for Pb, Sb, and Bi double-doping combinations with Mg_2Si . Figure 8 shows the values of the dimensionless figure-of-merit (ZT) for undoped and double-doped Mg_2Si . For all the undoped and doped Mg_2Si , the figure-of-merit increases with increasing temperature in the range from 323 K to 873 K. Tani and Kido reported maximum ZT values of approximately

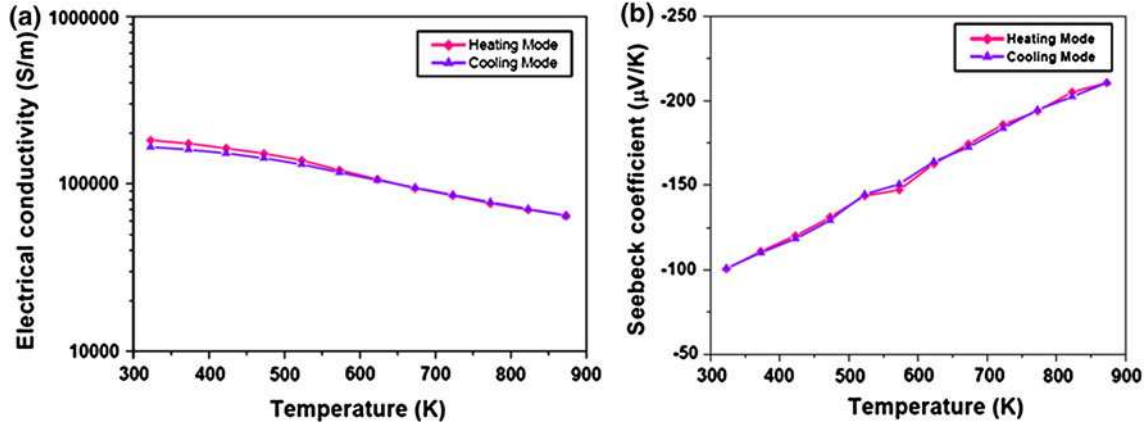


Fig. 5. Temperature dependence of (a) the electrical conductivity and (b) the Seebeck coefficient of double-doped Mg_2Si during heating and cooling.

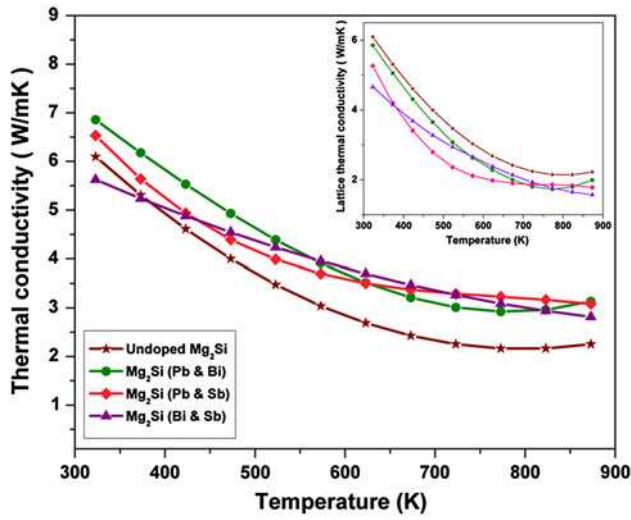


Fig. 6. Temperature dependence of the thermal conductivity of undoped and double-doped Mg_2Si . The inset shows the calculated lattice thermal conductivity.

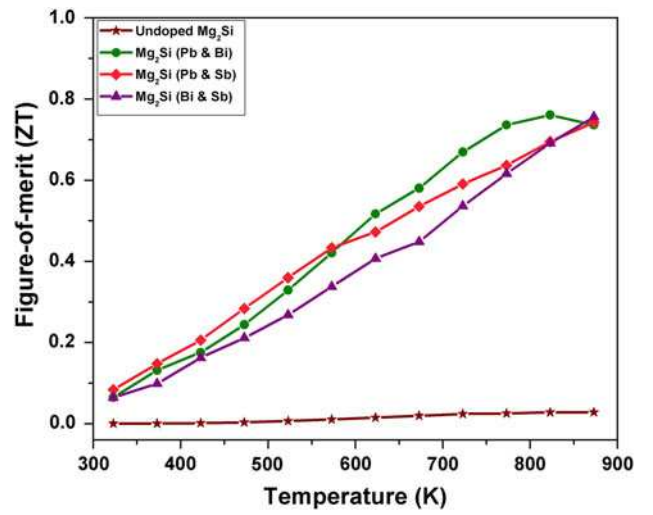


Fig. 8. Temperature dependence of the figure-of-merit of undoped and double-doped Mg_2Si .

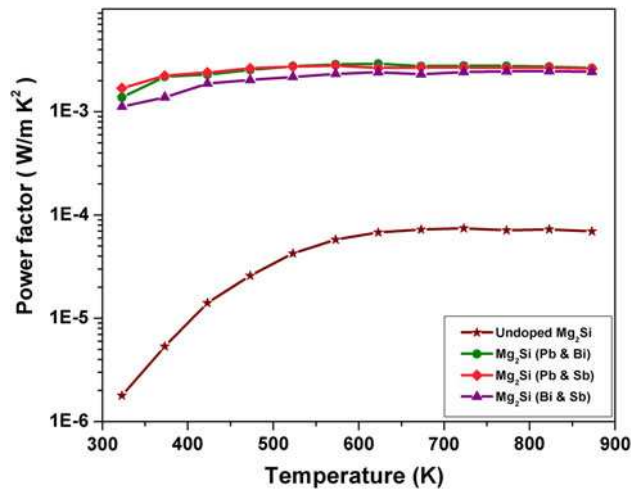


Fig. 7. Temperature dependence of the power factor of undoped and double-doped Mg_2Si

0.86 at 862 K for Bi-doped Mg_2Si ³ and approximately 0.56 at 862 K for Sb-doped Mg_2Si ⁴. Recently, Muthiah et al.¹⁹ reported a ZT value of approximately 0.56 at 873 K for Pb-doped Mg_2Si . Jung and Kim⁵ reported a ZT value of approximately 0.18 at 823 K for Te-doped Mg_2Si . In this study of double-doped Mg_2Si , ZT values were higher than for single-doped (Pb, Sb, or Te) Mg_2Si , although slightly lower than that of Bi-doped Mg_2Si . The ZT of the undoped sample in this study was calculated to be approximately 0.03 at 873 K whereas for double-doped Mg_2Si ZT was increased to approximately 0.7, irrespective of the doping combination used.

CONCLUSIONS

Double-doping studies of Mg_2Si have been conducted with Pb, Sb, and Bi as doping elements. Significant ZT enhancement of approximately 0.7 at 873 K was achieved by use of this double-doping

Double-Doping Approach to Enhancing the Thermoelectric Figure-of-Merit of n -Type Mg_2Si Synthesized by Use of Spark Plasma Sintering

approach, irrespective of the dopant combination used. This increase in ZT is primarily because of a significant increase in the electrical conductivity of the doped Mg_2Si . A small corresponding decrease in the Seebeck coefficient is also observed.

ACKNOWLEDGEMENTS

This work was supported by the CSIR-TAPSUN (Network Project NWP-54) programme entitled “Novel approaches for solar energy conversion under technologies and products for solar energy utilization through networking”. The authors are grateful to Radhey Shyam and N.K. Upadhyay for technical and experimental support.

REFERENCES

1. E. Savary, F. Gascoin, and S. Marinel, *Dalton Trans.* 39, 11074 (2010).
2. J.J. Pulikkotil, D.J. Singh, S. Auluck, M. Saravanan, D.K. Misra, A. Dhar, and R.C. Budhani, *Phys. Rev. B* 86, 155204 (2012).
3. J.I. Tani and H. Kido, *Phys. B* 364, 218 (2005).
4. J.I. Tani and H. Kido, *Intermetallics* 15, 1202 (2007).
5. J.Y. Jung and I.H. Kim, *J. Electron. Mater.* 40, 1144 (2011).
6. J.I. Tani and H. Kido, *J. Alloys Compd.* 466, 335 (2008).
7. Q.S. Meng, W.H. Fan, R.X. Chen, and Z.A. Munir, *J. Alloys Compd.* 509, 7922 (2011).
8. T. Sakamoto, T. Iida, A. Matsumoto, Y. Honda, T. Nemoto, J. Sato, T. Nakajima, H. Taguchi, and Y. Takanashi, *J. Electron. Mater.* 39, 1708 (2010).
9. M. Akasaka, T. Iida, A. Matsumoto, K. Yamanaka, Y. Takanashi, T. Imai, and N. Hamada, *J. Appl. Phys.* 104, 013703 (2008).
10. H.I. Mouko, C. Mercier, J. Tobola, G. Pont, and H. Scherrer, *J. Alloys Compd.* 509, 6503 (2011).
11. J.I. Tani and H. Kido, *Intermetallics* 32, 72 (2013).
12. Y. Niwa, Y. Todaka, T. Masuda, T. Kawai, and M. Umemoto, *Mater. Trans.* 50, 1725 (2009).
13. X. Zhou, G. Wang, H. Chi, X. Su, J.R. Salvador, W. Liu, X. Tang, and C. Uher, *J. Electron. Mater.* 41, 1589 (2012).
14. V.K. Zaitsev, M.I. Fedorov, E.A. Gurieva, I.S. Eremin, P.P. Konstantinov, A.Y. Samunin, and M.V. Vedernikov, *Phys. Rev. B* 74, 045207 (2006).
15. Q. Zhang, J. He, T.J. Zhu, S.N. Zhang, X.B. Zhao, and T.M. Tritt, *Appl. Phys. Lett.* 93, 102109 (2008).
16. W. Liu, X. Tan, K. Yin, H. Liu, X. Tang, J. Shi, Q. Zhang, and C. Uher, *Phys. Rev. Lett.* 108, 166601 (2012).
17. X. Zhang, Q.M. Lu, L. Wang, and F.P. Zhang, *J. Electron. Mater.* 39, 1413 (2010).
18. D. Cederkrantz, N. Farahi, K.A. Borup, B.B. Iversen, M. Nygren, and A.E.C. Palmqvist, *J. Appl. Phys.* 111, 023701 (2012).
19. S. Muthiah, J. Pulikkotil, A.K. Srivastava, A. Kumar, B.D. Pathak, A. Dhar, and R.C. Budhani, *Appl. Phys. Lett.* 103, 053901 (2013).